

COMMUNICATION

Surface-engineered nanomaterials as X-ray absorbing adjuvant agents for Auger-mediated chemo-radiation†

Cite this: *Nanoscale*, 2013, 5, 5252

Sang-Min Lee,^{‡,ab} De-Hao Tsai,^a Vincent A. Hackley,^a Martin W. Brechbiel^b and Robert F. Cook^{*a}

Received 18th January 2013

Accepted 11th April 2013

DOI: 10.1039/c3nr00333g

www.rsc.org/nanoscale

We report a prototype approach to formulate gold nanoparticle-based X-ray absorbing agents through surface-engineering of a cisplatin pharmacophore with modified polyacrylate. The resulting agents exhibit both chemo-therapeutic potency to cancer cells and Auger-mediated secondary electron emission, showing great potential to improve the therapeutic efficacy of chemo-radiation.

Surface-engineered nanomaterials, and their derivative products, are highly attractive candidates for therapeutic applications. The advantages of using these constructs arise primarily from their nanoscale dimensions and controllable surface chemistry, allowing selective delivery of an incorporated payload to a tumor interstitium *via* leaky vasculature, while avoiding systemic clearance through renal filtration. The improved therapeutic window and enhanced pharmacokinetic profiles, for example, have demonstrated substantial potential for applications in anticancer drugs and tumor imaging agents.^{1,2}

Among diverse surface-engineered nanomaterials attempted to address nanostructure–biological activity relationships, functionalized gold nanoparticles (AuNPs) are considered one of the most important,^{3,4} primarily due to their intrinsically non-toxic nature, good redox stability, specific surface plasmon resonance (SPR) bands, and facile surface chemistry. As a result, AuNPs have been widely exploited for a variety of biomedical applications including delivery of small-interfering RNA,^{5,6} pharmaceuticals,^{7–9} imaging agents,^{10,11} facilitation of computed tomography,¹² surface-enhanced Raman scattering imaging, and photothermal therapy.^{13–15}

Using secondary electron emission from AuNPs,^{16,17} recent developments suggest an exciting potential for using AuNPs to enhance the X-ray dosage at the target site in radiation therapy. Based on this concept, the Auger-type electron emission should have the capacity to deliver sufficient doses of highly localized energy to the cellular organelles (*e.g.*, DNA in nuclear chromosomes) and to induce substantial damage to the targeted cells.^{18–20} Furthermore, because of their rapid decay in nanoscale volumes, the linear-energy-transfer properties of Auger electrons may prevent damage to the surrounding healthy tissue.²¹ Moreover, the overall therapeutic performance can be further improved conceptually by incorporating intelligent and complementary design principles.

Herein, we demonstrate an approach to develop and combine chemo- and radiation-therapeutic modalities. Our approach involves engineering of a cisplatin pharmacophore (Pt^{II}) onto the surface of stable AuNPs. Beyond the known chemotherapeutic potency,^{22,23} the Pt^{II}-based treatment regimens have also been synchronized with external radiation for inducing additional DNA damage and to interfere with post-radiation DNA-repair processes.^{24,25} The concept of formulating the (Pt^{II} + AuNP) drug complex has also spurred development of a Pt^{II}-radiosensitizer for concurrent chemo-radiation therapy.^{25,26} Moreover, the AuNP-based therapeutic agent demonstrated in this study provides a relevant test bed for development and validation of quantitative measurements for biomedically related functionalized nanoscale materials.

Although the notion of this nanoplateform-mediated delivery (Pt^{II} + AuNPs) provides a highly promising strategy for cancer treatments, an obvious challenge thus far has been to accurately engineer this nanomaterial platform on demand to achieve the desired biological functionality. Therefore, understanding the surface chemistry of nanomaterials is of crucial importance in order to optimize the material performance for biomedical applications.

To fabricate surface-tailored Pt^{II}-AuNPs, poly(acrylic acid) (PAA) was first adhered to the Au surface *via* lipoic acid anchor groups.²⁷ Subsequently Pt^{II} pharmacophores were bound to the

^aMaterial Measurement Laboratory, National Institute of Standards and Technology, Gaithersburg, Maryland 20899, USA. E-mail: robert.cook@nist.gov

^bNational Cancer Institute, National Institutes of Health, Bethesda, Maryland 20892, USA

† Electronic supplementary information (ESI) available: Experimental procedure. See DOI: 10.1039/c3nr00333g

‡ Current address: Department of Chemistry, The Catholic University of Korea, Bucheon, Gyeonggi-do 420-743, Korea.

PAA through metal–carboxylate coordination^{28,29} (Scheme 1). Such a formulation allows for a high loading capacity with respect to Pt^{II} pharmacophores (more than 1300 Pt^{II} ions per particle, see ESI†) without significant aggregation of the AuNPs. More importantly, a moderate amount of Pt^{II}-mediated multi-dentate binding can cross-link polymer networks on the surface of individual AuNPs. This cross-linking should increase the robustness of PAA chains on the AuNP surface and thereby provide improved colloidal and conjugate stability.³⁰ This would be particularly useful to facilitate the Pt^{II} pharmacophore release to solid tumor tissue under acidic conditions.³¹ To this end, our work begins from the foundation of multiple complementary characterization approaches in order to understand the chemical formulation of the drug-tethered nanoplatform, prior to the study of Auger-mediated radiotherapy and *in vitro* chemotherapeutic efficacy.

Lipoic PAA ($M_n = 2.4$ kDa) was prepared *via* amide coupling of lipoic acid with poly(*tert*-butyl acrylate) followed by acidolysis (details in the ESI†). Then, a 4-fold excess of lipoic PAA (compared to the available surface atoms of AuNPs³²) was reacted with tannic acid-stabilized (referred to here as ‘native’) AuNPs (zeta potential, $\zeta = -24.4$ mV \pm 4.3 mV, hydrodynamic diameter, $D_H = 10.4$ nm \pm 1.9 nm) and stirred overnight to yield PAA-modified AuNPs. (All reported uncertainties represent one standard deviation calculated from at least three replicate measurements.) This was followed by dialysis to remove unreacted species (PAA–AuNPs, $\zeta = -64.7$ mV \pm 5.4 mV, $D_H = 25.1$ nm \pm 3.9 nm in Fig. 1A). Pt^{II}-conjugation was achieved by the incubation of PAA–AuNP suspension with the Pt^{II} pharmacophore, *cis*-[Pt(NH₃)₂(H₂O)₂]²⁺ in different Pt^{II}-to-AuNP ratios (*i.e.*, the number of Pt^{II} atoms per AuNP, on average, defined as Ω) at 25 °C and purified by a centrifugal filter. ¹H NMR spectra exhibited the initial binding of Pt^{II} ions to PAA with downshifted proton peaks from the PAA backbone on Pt^{II} coordination (Fig. 2A, $\Omega = 1300$ as representative). The apparent ζ of Pt^{II}-AuNPs was increasingly neutralized as the degree of Pt^{II}-conjugation increased, yielding values of (-54.3 ± 4.3) mV and (-50.5 ± 4.8) mV for Ω of 700 and 1300, respectively, while D_H decreased to (21.2 \pm 4.4) nm and (18.9 \pm 3.3) nm, respectively (Fig. 1A). The electrophoretic mobility of PAA–AuNPs and Pt^{II}-AuNPs in agarose gel on Pt^{II}-conjugation (Fig. 1B) was not differentiable, confirming a compensation of decreasing size

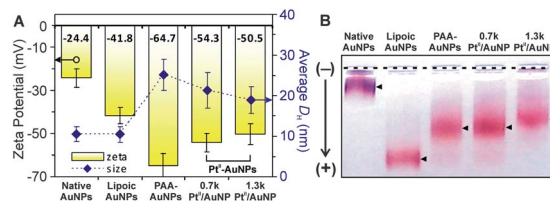
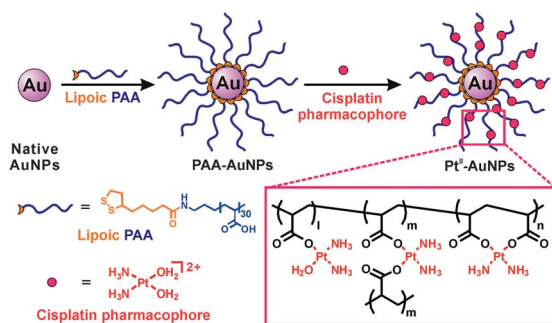


Fig. 1 (A) Zeta potential and average hydrodynamic diameter (D_H) of native AuNPs, lipoic acid-modified AuNPs (lipoic AuNPs), PAA–AuNPs, and Pt^{II}-AuNPs with 0.7k and 1.3k Pt^{II}/AuNP ratios (Ω). (B) The corresponding electrophoretic migration of modified AuNPs in 3% agarose gel (150 V, 60 min).

with charge neutralization (as observed in Fig. 1A).³³ The size contraction can be attributed to the Pt^{II}-mediated cross-linking of surface-bound PAA chains (*vide infra*).

Next we evaluated the colloidal stability of the Pt^{II}-AuNP vector. Using the concept of Derjaguin, Landau, Verwey and Overbeek theory, the presence of Pt^{II} in aqueous solution can significantly reduce the colloidal stability of unprotected AuNPs by shielding the charge repulsion between the particles.³⁴ Indeed, during the Pt^{II}-conjugation reaction, only PAA–AuNPs exhibited the characteristic SPR peak wavelength at 520 nm without any spectral changes. Both native AuNPs and lipoic-conjugated AuNPs exhibited a significant red-shift in their SPR spectra (Fig. 2B) due to the ion-mediated particle aggregation. The results confirm that the surface-bound PAA chains provide essential strong electrostatic repulsion and steric hindrance to ensure the AuNPs stability on the addition of Pt^{II} ions. Furthermore, the colloidal stability of Pt^{II}-AuNPs was maintained even under high ionic strength in cell culture media (Eagle's Minimum Essential Medium), with no change in the SPR band (Fig. 2B). Formation of nanoparticle aggregates is known to significantly impact the cellular uptake properties.³⁵ Such an enhanced colloidal stability of the Pt^{II}-AuNP formulation (*i.e.*, containing lipoic PAA) is critical for subsequent *in vitro* studies. Note that massive aggregation of AuNPs was observed when $\Omega > 2500$, due to interparticle cross-linking⁹ mediated by excessive Pt^{II} ions (Table S2 and Fig. S2B in the ESI†).

Given the apparent stable formation of Pt^{II}-AuNPs, as indicated by the characteristic SPR band, and with a desire to further elucidate the binding mechanism of Pt^{II} on lipoic-PAA-functionalized AuNPs, we utilized attenuated total reflectance-Fourier transform infrared (ATR-FTIR) spectroscopy and X-ray



Scheme 1 Preparation of cisplatin pharmacophore-tethered gold nanoparticles (Pt^{II}-AuNPs).

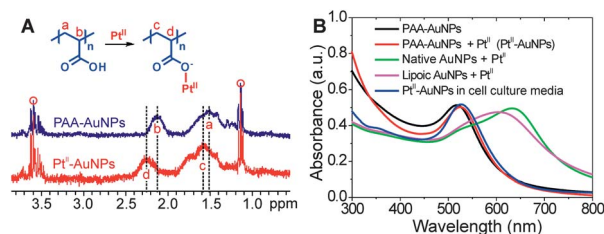


Fig. 2 (A) ¹H NMR spectra of PAA–AuNPs and Pt^{II}-AuNPs. The circled peaks are due to the trace amount of ethanol, added to D₂O as a reference. (B) SPR spectra of AuNPs measured by UV-vis absorption.

photoelectron spectroscopy (XPS). Compared to the conventional FTIR method, the evanescent waves present in the ATR element allows for much greater sensitivity to surface-bound species³⁶ (Fig. 3A, left inset). As shown in Fig. 3A, PAA–AuNPs exhibit the characteristic C=O stretching peak at 1703 cm^{-1} associated with the carboxyl group in PAA, while negligible absorbance was observed from COO[−] anti-symmetric stretching at 1552 cm^{-1} . On the addition of Pt^{II} ions, the peak intensities for both anti-symmetric (1552 cm^{-1}) and symmetric (1409 cm^{-1}) COO[−] stretching increased while the C=O peak intensity decreased; these effects can be attributed to Pt^{II} coordination with the COO[−] ligands.³⁷ Given that the Pt^{II}–AuNP suspension was kept slightly acidic to prevent the agglomeration of Pt^{II} ions through (μ^2 -OH) ligand bridging,³⁸ the appearance of COO[−] peaks can only be attributed to Pt^{II}-coordination rather than base-mediated simple deprotonation of PAA. Also the relative ratio of peak intensities ($r = I(\text{COO}^-)_{\text{anti}}/I(\text{C}=\text{O})$) in Fig. 3A) increases as additional Pt^{II} ions are conjugated, further supporting Pt^{II}-coordination as discussed above.

In stark contrast to the spectrum for the carboxylate group, which generally shows a stronger anti-symmetric *versus* symmetric peak³⁹ (Fig. S4 in the ESI[†]), Pt^{II}–AuNPs exhibit the reverse pattern. This is likely attributable to bidentate binding of COO[−] ligands with Pt^{II} ions rather than monodentate binding, as previously reported.³⁷ Additionally, due to the large size of the Pt^{II} ion, bidentate bridging complexes have been more commonly observed than the chelating Pt^{II}–carboxylate compounds (Scheme S2 in the ESI[†])³⁸ Hence, it is postulated that PAA polymer chains can be cross-linked by Pt^{II}-coordination (Fig. 3A, right inset), leading to size contraction of Pt^{II}–AuNPs as shown in Fig. 1A. Indeed, such bidentate bridging

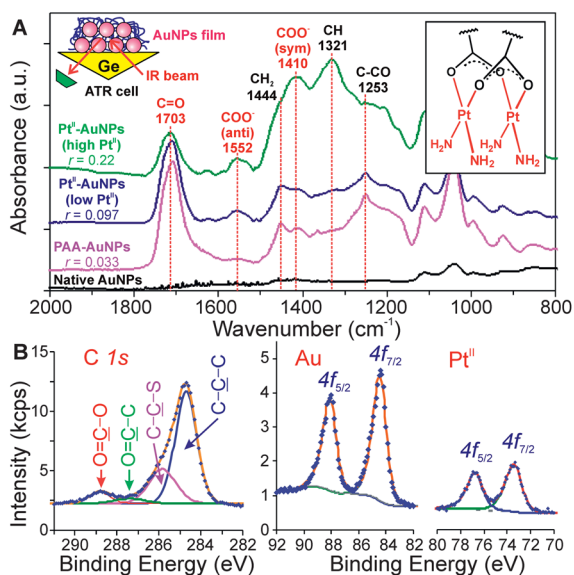


Fig. 3 (A) Attenuated total reflectance-Fourier transform infrared (ATR-FTIR) spectra of tannic acid-stabilized (native) AuNPs, PAA–AuNPs, and Pt^{II}–AuNPs with Pt^{II}/AuNP ratios of 0.7k (low Pt^{II}) and 1.3k (high Pt^{II}). The intensity ratio (r) was determined by the ratio of the intensity of (COO[−])_{anti} to the intensity of (C=O). Left inset: schematic picture of the Ge crystal ATR cell, where AuNP samples were deposited by drop-casting. Right inset: possible Pt^{II}-binding mode on PAA in Pt^{II}–AuNPs. (B) XPS spectra for C 1s, Au 4f, and Pt 4f regions collected from Pt^{II}–AuNPs.

cisplatin–acetate compounds are readily formed with their crystal structure being firmly resolved.²⁹ As such, the observation indicates that PAA polymer chains allow for the efficient loading of Pt^{II} ions on AuNPs, which should enhance the colloidal stability *via* cross-linking with the pharmacophores protected in the matrix of PAA chains. Eventually, this binding mode can lead to the release of the Pt^{II} pharmacophore at target sites on triggering under acidic conditions generally associated with solid tumor tissue³¹ (Fig. S6 in the ESI[†]).

XPS results provide complementary information on the chemical environment associated with Pt^{II}–PAA binding in Pt^{II}–AuNPs. Fig. 3B shows high-resolution regional scans of C 1s, Au 4f, and Pt 4f peaks, closely matching the binding energy of each element in the Pt^{II}–AuNPs vector: lipoic–PAA, AuNP, and Pt^{II}, respectively. Specifically, the Pt 4f region shows a pair of peaks for 4f_{5/2} (76.9 eV) and 4f_{7/2} (73.6 eV) from Pt^{II} ions with little shift (<0.5 eV) from those of cisplatin⁴⁰ (73.3 eV for 4f_{7/2}), indicating no change in the oxidation state of Pt^{II} pharmacophores tethered on PAA–AuNPs.⁴¹ Note that the ratio of Pt^{II} to AuNP measured by XPS is about six times greater than the \mathcal{Q} value in the actual formulation. As the penetration depth of the X-rays was only $\approx 10\text{ nm}$, there was greater sensitivity to the Pt^{II} ions located on the top layer than the Au surface beneath. Details of the XPS analysis are described in the ESI[†].

Auger-mediated secondary electrons figure prominently for radiation therapy, as discussed previously. To evaluate the performance of our Pt^{II}–AuNPs as an Auger-emitting adjuvant agent, we monitored the secondary electron emission using non-monochromated Bremsstrahlung radiation, a virtual X-ray source for external radiation. As shown in Fig. 4, Auger electron peaks from both Au and Pt^{II} are indeed observed in the kinetic energy spectrum. The results clearly correspond closely to the Auger lines of each element, and are consistent with their Auger parameters⁴⁰ (Table S1 in the ESI[†]). Although the peak intensities are not sufficiently great due to the low relative sensitivity factor of Auger emission, a single photoelectron emission event can trigger the emission of numerous secondary electrons from the outer shells in high- z elements such as Au and Pt^{II}. Our results provide a proof of concept for the potential as an adjuvant agent for radiation therapy.

In addition to radiation-mediated Auger lines, the *in vitro* chemotherapeutic potency of Pt^{II}–AuNPs was also evaluated with MCF-7 breast cancer and SKOV-3 ovarian cancer cell lines, both of which were known to be partially resistant to cisplatin (Fig. 5). After 48 h and 72 h treatments using both cell lines,

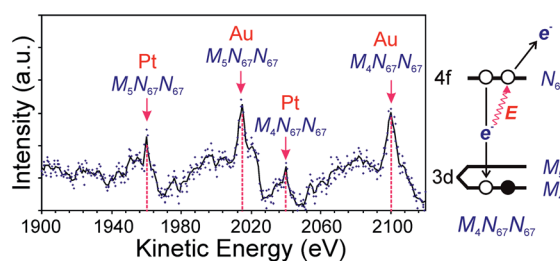


Fig. 4 Electron kinetic energy spectrum of Auger emission from Pt^{II}–AuNPs. Each peak was identified by comparing to the NIST XPS Database.⁴⁰

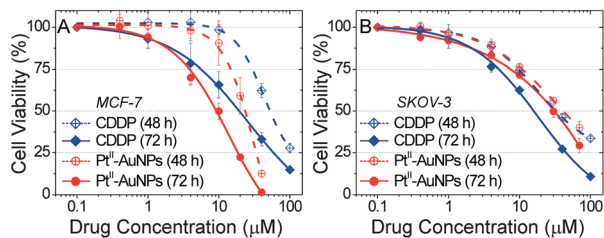


Fig. 5 *In vitro* cytotoxicity profiles of Pt^{II}-AuNPs and cisplatin (CDDP) with MCF-7 breast cancer and SKOV-3 ovarian cancer cells.

significant cytotoxicity was observed for Pt^{II}-AuNPs, which shows comparable potency to that of the cisplatin parent drug (*i.e.*, 20 and 70 µM of Pt^{II}-AuNPs for less than 30% of cell viability for MCF-7 and SKOV-3, respectively, after 72 h). Given the acid-triggered release of the Pt^{II} pharmacophore observed with Pt^{II}-AuNPs (Fig. S6 in the ESI[†]), such a chemotherapeutic potency can be attributed to the endocytosis-mediated cellular uptake process of nanomaterials as previously reported,^{8,9} subsequently leading to the triggered drug-release in acidic endosomal environments.⁴² In contrast, PAA-AuNPs without the Pt^{II}-pharmacophore exhibit negligible cytotoxicity after 3 days (Fig. S7 in the ESI[†]).

In conclusion, Pt^{II} pharmacophore-tethered AuNPs can be synthesized *via* lipophilic acid-terminated multidentate PAA chains. Through careful examination by multiple and complementary characterization methods, therapeutic responses of Pt^{II}-AuNPs can be correlated with their surface properties accurately. Both the drug loading and colloidal stability can be enhanced significantly by bidentate bridging of PAA to Pt^{II} on AuNPs. *In vitro* chemotherapeutic assays confirm the potency of Pt^{II}-AuNPs with MCF-7 breast cancer and SKOV-3 ovarian cancer cell lines. In addition, Auger electron emissions triggered by external ionizing radiation demonstrate the therapeutic potential of Pt^{II}-AuNP as an X-ray absorbing adjuvant agent for chemo-radiation cancer therapy. As such, the Pt^{II}-AuNP-mediated therapeutic synergy in concurrent chemo-radiation will be evaluated in due course.

Acknowledgements

This work was performed while S.-M. Lee held a National Research Council Postdoctoral Research Fellowship jointly with the National Institute of Standards and Technology (NIST) and National Institutes of Health (NIH). The authors thank Drs Jacek Capala and Kwon Joong Yong at NIH, Dr Tae Joon Cho for internal review at NIST, and Dr Jiwen Zheng at the Food and Drug Administration for TEM analyses.

Notes and references

- 1 D. Peer, J. M. Karp, S. Hong, O. C. Farokhzad, R. Margalit and R. Langer, *Nat. Nanotechnol.*, 2007, **2**, 751–760.
- 2 M. E. Davis, Z. Chen and D. M. Shin, *Nat. Rev. Drug Discovery*, 2008, **7**, 771–782.
- 3 M. A. Dobrovolskaia, P. Aggarwal, J. B. Hall and S. E. McNeil, *Mol. Pharmaceutics*, 2008, **5**, 487–495.

- 4 E. Boisselier and D. Astruc, *Chem. Soc. Rev.*, 2009, **38**, 1759–1782.
- 5 J.-S. Lee, J. J. Green, K. T. Love, J. Sunshine, R. Langer and D. G. Anderson, *Nano Lett.*, 2009, **9**, 2402–2406.
- 6 D. A. Giljohann, D. S. Seferos, A. E. Prigodich, P. C. Patel and C. A. Mirkin, *J. Am. Chem. Soc.*, 2009, **131**, 2072–2073.
- 7 J. D. Gibson, B. P. Khanal and E. R. Zubarev, *J. Am. Chem. Soc.*, 2007, **129**, 11653–11661.
- 8 S. Dhar, W. L. Daniel, D. A. Giljohann, C. A. Mirkin and S. J. Lippard, *J. Am. Chem. Soc.*, 2009, **131**, 14652–14653.
- 9 S. D. Brown, P. Nativo, J.-A. Smith, D. Stirling, P. R. Edwards, B. Venugopal, D. J. Flint, J. A. Plumb, D. Graham and N. J. Wheate, *J. Am. Chem. Soc.*, 2010, **132**, 4678–4684.
- 10 C. Alric, J. Taleb, G. L. Duc, C. Mandon, C. Billotey, A. L. Meur-Herland, T. Brochard, F. Vocanson, M. Janier, P. Perriat, S. Roux and O. Tillement, *J. Am. Chem. Soc.*, 2008, **130**, 5908–5915.
- 11 Y. Song, X. Xu, K. W. MacRenaris, X.-Q. Zhang, C. A. Mirkin and T. J. Meade, *Angew. Chem., Int. Ed.*, 2009, **121**, 9307–9311.
- 12 D. Kim, S. Park, J. H. Lee, Y. Y. Jeong and S. Jon, *J. Am. Chem. Soc.*, 2007, **129**, 7661–7665.
- 13 P. K. Jain, X. Huang, I. H. El-Sayed and M. A. El-Sayed, *Acc. Chem. Res.*, 2008, **41**, 1578–1586.
- 14 Y. Xia, W. Li, C. M. Cobley, J. Chen, X. Xia, Q. Zhang, M. Yang, E. C. Cho and P. K. Brown, *Acc. Chem. Res.*, 2011, **44**, 914–924.
- 15 T. W. Odom and G. C. Schatz, *Chem. Rev.*, 2011, **111**, 3667–3668.
- 16 J. D. Carter, N. N. Cheng, Y. Qu, G. D. Suarez and T. Guo, *J. Phys. Chem. B*, 2007, **111**, 11622–11625.
- 17 A. K. Pradhan, S. N. Nahar, M. Montenegro, Y. Yu, H. L. Zhang, C. Sur, M. Mroziak and R. M. Pitzer, *J. Phys. Chem. A*, 2009, **113**, 12356–12363.
- 18 B. Boudaïffa, P. Cloutier, D. Hunting, M. A. Huels and L. Sanche, *Science*, 2000, **287**, 1658–1660.
- 19 C. A. Boswell and M. W. Brechbiel, *J. Nucl. Med.*, 2005, **46**, 1946–1947.
- 20 T. Kong, J. Zeng, X. Wang, X. Yang, J. Yang, S. McQuarrie, A. McEwan, W. Roa, J. Chen and J. Z. Xing, *Small*, 2008, **4**, 1537–1543.
- 21 J. F. Hainfeld, F. A. Dilmanian, D. N. Slatkin and H. M. Smilowitz, *J. Pharm. Pharmacol.*, 2008, **60**, 977–985.
- 22 D. Wang and S. J. Lippard, *Nat. Rev. Drug Discovery*, 2005, **4**, 307–320.
- 23 L. Kelland, *Nat. Rev. Cancer*, 2007, **7**, 573–584.
- 24 T. Y. Seiwert, J. K. Salama and E. E. Vokes, *Nat. Clin. Pract. Oncol.*, 2007, **4**, 86–100.
- 25 P. G. Rose, *Nat. Clin. Pract. Oncol.*, 2011, **8**, 388–390.
- 26 J. Rousseau, C. Boudou, R. F. Barth, J. Balosso, F. Estève and H. Elleaume, *Clin. Cancer Res.*, 2007, **13**, 5195–5201.
- 27 M. H. Stewart, K. Susumu, B. C. Mei, I. L. Medintz, J. B. Delehanty, J. B. Blanco-Canosa, P. E. Dawson and H. Mattoussi, *J. Am. Chem. Soc.*, 2010, **132**, 9804–9813.
- 28 M. J. Han, T. J. Cho, S. J. Park, Y. S. Sohn, C. O. Lee and S. U. Choi, *J. Bioact. Compat. Polym.*, 1992, **7**, 358–369.

- 29 K. Sakai, M. Takeshita, Y. Tanaka, T. Ue, M. Yanagisawa, M. Kosaka, T. Tsubomura, M. Ato and T. Nakano, *J. Am. Chem. Soc.*, 1998, **120**, 11353–11363.
- 30 B. A. Kairdolf and S. Nie, *J. Am. Chem. Soc.*, 2011, **133**, 7268–7271.
- 31 I. F. Tannock and D. Rotin, *Cancer Res.*, 1989, **49**, 4373–4384.
- 32 R. I. MacCuspie, A. M. Elsen, S. J. Diamanti, S. T. Patton, I. Altfeder, J. D. Jacobs, A. A. Voevodin and R. A. Vaia, *Appl. Organomet. Chem.*, 2010, **24**, 590–599.
- 33 T. L. Doane, Y. Cheng, A. Babar, R. J. Hill and C. Burda, *J. Am. Chem. Soc.*, 2010, **132**, 15624–15631.
- 34 D.-H. Tsai, L. F. Pease III, R. A. Zangmeister, M. J. Tarlov and M. R. Zachariah, *Langmuir*, 2009, **25**, 140–146.
- 35 E. C. Cho, Q. Zhang and Y. Xia, *Nat. Nanotechnol.*, 2011, **6**, 385–391.
- 36 D.-H. Tsai, M. Davila-Morris, F. W. DelRio, S. Guha, M. R. Zachariah and V. A. Hackley, *Langmuir*, 2011, **27**, 9302–9313.
- 37 J. Petroski and M. A. El-Sayed, *J. Phys. Chem. A*, 2003, **107**, 8371–8375.
- 38 T. G. Appleton, R. D. Berry, C. A. Davis, J. R. Hall and H. A. Kimlin, *Inorg. Chem.*, 1984, **23**, 3514–3521.
- 39 L. J. Kirwan, P. D. Fawell and W. van Bronswijk, *Langmuir*, 2003, **19**, 5802–5807.
- 40 NIST XPS Database, <http://www.srdata.nist.gov/xps/Default.aspx>, accessed January 2012.
- 41 For comparison, Pt ($4f_{7/2}$) peaks range at 75–77 eV for Pt^{IV} compounds and 70–71 eV for Pt⁰ compounds. Please see ESI.†
- 42 J. R. Casey, S. Grinstein and J. Orłowski, *Nat. Rev. Mol. Cell Biol.*, 2010, **11**, 50–61.